Bulletin of Earth Sciences of Thailand

Acid Forming Potential of Black Shale in Ban Pong Basin, Northern Thailand

Nachayada Phonseela[1]*, Thitiphan Assawincharoenkij[2], Sirilak Lorchuenwong[2]

[1] M.Sc. Petroleum Geoscience Program, Department of Geology, Faculty of Science, Chulalongkorn University, Bangkok, 10330, Thailand
[2] Department of Geology, Faculty of Science, Chulalongkorn University, Bangkok, 10330, Thailand
*Corresponding author e-mail: nachayada.bt@gmail.com

Received: 15 Jun 2022
Revised: 19 Jul 2022
Accepted: 19 Jul 2022

Abstract

The black shale and exposed rocks located at an open-pit mine in the Ban Pong Basin, Chiang Mai province, northern Thailand, have been studied to evaluate acid forming potential using acid-base accounting and net acid generation tests. The mine water chemistry was also investigated to observe the potential of acid mine drainage. The results present that pyrite is found in pale brown marlstone, coaly black shale, and black shale with fossil fragments, whereas calcite is observed in all rock types except for coaly black shale. The acid forming potential outcomes show that only the coaly black shale is classified as an acid forming rock because of high pyrite content, while other rocks are categorized as non-acid forming rocks due to the absence of pyrite and/or elevated calcite content. Moreover, the neutral pH and low metal concentration of mine water indicate no acid mine drainage potential in the study area. The hydrochemical facies of water was classified as Ca-Mg-HCO_3 type for upstream and downstream of Ca-Mg-SO_4 type for mine water. The enrichment of Ca, Mg, and HCO_3 in the surface water is attributed to weathering of carbonate material of the surrounding rocks. In contrast, the dominance of SO_4 in mine water is perhaps influenced by pyrite oxidation and gypsum dissolution. To summarize, the coaly black shale is an acid forming rock, but it does not produce acid mine drainage since it is surrounded by calcite-rich rocks acting as the acid neutralizer.

Keywords: acid mine drainage, pyrite oxidation, hydrochemical facies, mine water, surface water

1. Introduction

Black shale is a dark-colored, fine-grained, thin-bedded sedimentary rock enriched with pyrite and organic matter (Kwong et al., 2009). It is typically deposited in bottom water and/or bottom sediment under an anoxic condition in marine and continental sedimentary basins (Huyck, 1990; Kontinen, 2015; Wignall, 1994). When black shale outcrops are exposed to oxic conditions, sulfide minerals are sensitive to oxidation and dissolution (Equeenuddin et al., 2010). Consequently, protons and trace metals are liberated, leading to acid mine drainage (AMD) (Jambor et al., 2000) — one of the world's most significant environmental problems regarding mining (Changul et al., 2010a). The AMD will decrease pH and mobilize toxic metal(loid)s, impacting aquatic biota and degrading surface and groundwater quality (Nordstrom, 1997; Strosnider, 2011a; Strosnider, 2011b; Sun et al., 2013). Furthermore, due to the abundance of harmful elements in black shales, they possibly have a potential source of soil, groundwater, and surface water contamination (Parviainen and Loukola-Ruskeeniemi, 2019).

When pyrite is oxidized by oxygen and water (Eq. 1), sulfate (SO_4^{2-}), ferrous iron (Fe^{+2}), and two moles of protons (H^+) for each mole of oxidized pyrite are generated in the system. Then the produced ferrous iron will be oxidized (Eq.2), turning to ferric iron (Fe^{+3}), which acts as an oxidizing agent for pyrite (Eq.3) (Lottermoser, 2010). If pyrite is oxidized by ferric iron (Eq. 3), 16 mol of protons will be liberated per mole of pyrite oxidized.

$$FeS_2 + \frac{7}{2}O_2 + H_2O \rightarrow Fe^{2+} + 2SO_4^{-2} + 2H^+ \quad \text{.....(1)}$$

$$Fe^{2+} + \frac{1}{4}O_2 + H^+ \rightarrow Fe^{3+} + \frac{1}{2}H_2O \quad \text{.....(2)}$$

$$FeS_2 + 14Fe^{3+} + 8\,H_2O \rightarrow 15\,Fe^{2+} + 2SO_4^{-2} + 16H^+ \quad \text{...(3)}$$

Herein, this study focuses on a section of Miocene fine-grained sedimentary rock (Adisaipattanakul, 2014) at an open-pit mine in the Ban Pong Basin (the BPB), Chiang Mai province, northern Thailand (Fig. 1). The

purpose of this mine is to produce the soil for sale. The section of interest (Fig. 2) contains thick light gray mudstone, coaly black shale interbedded with marlstone, and black shale with fossil fragments interbedded with marlstone. Since mining operation allows the rocks to be exposed to oxidative conditions, this might lead to AMD. Therefore, this study aims (1) to evaluate the acid forming potential of black shale and exposed rocks using acid-base accounting and net acid generation tests and (2) to observe acid mine drainage potential on mine water.

2. Geological setting

The Ban Pong Basin (BPB) is a N-S striking Cenozoic intermountain basin located in a synform in between two granite-gneissic terrains (Sutep-Inthanon mountain range) of the western metamorphic complex on the western side of Chiang Mai Basin (Fig. 3) (Mankhemthong et al., 2019). The basin was formed on the hanging wall of low-angle normal fault (LNF), known as Inthanon detachment (Mankhemthong et al., 2019), and was filled with semi-consolidated sediments of Miocene Mae Rim Formation (Adisaipattanakul, 2014). The formation consists of three lithofacies (from the older to the younger units): (1) a lower fluvial-alluvial unit, (2) a lacustrine unit and (3) an upper fluvial-alluvial unit (Adisaipattanakul, 2014). The Mae Rim Formation in the BPB dips towards the west and overlies the basement rocks, including metamorphosed limestone, shale, sandstone, and chert of Paleozoic rocks (Adisaipattanakul, 2014). Moreover, Rhodes et al. (2000) suggested that the Mae Rim Formation's provenance comes from the older Paleozoic units.

3. Methodology

3.1 Data sampling

In March and April 2022, field data collection was performed at the open-pit operated in the Ban Pong Basin. First, a lithostratigraphic log was executed to identify rock types. Then, nine rock samples of four lithologies were gathered, including calcareous light gray mudstone, pale brown marlstone, coaly black shale, and black shale with fossil fragments. The rock sampling interval is shown in the lithostratigraphic log (Figure 4).

Furthermore, three surface water samples were collected: upstream, mine water, and downstream (Fig. 1). The pH of the water sample was measured immediately from the non-filtered samples before separating the sample into three subsamples.

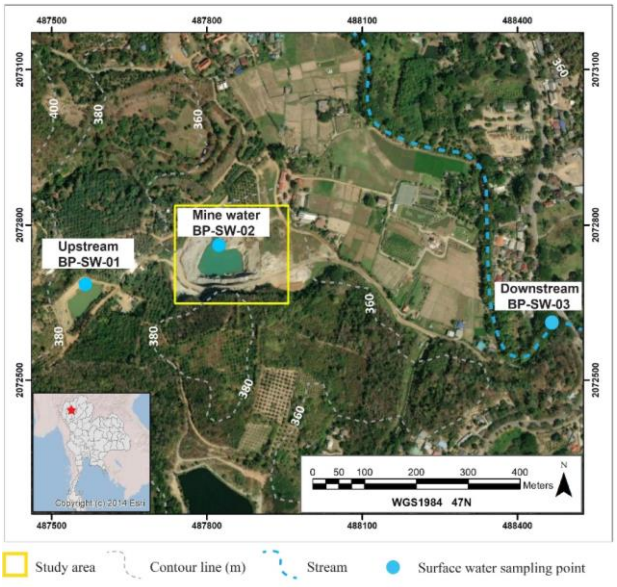

Figure 1 The study area is situated at the open-pit mine operation in the BPB, Chiang Mai province, northern Thailand. The blue circles represent the location of surface water sampling upstream, mine water, and downstream.

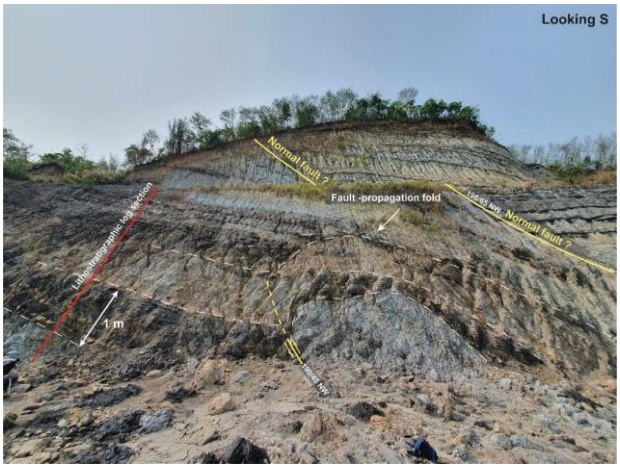

Figure 2 The section of interest contains coaly black shale and black shale with fossil fragments interbedded with pale brown marlstone and light gray calcareous mudstone. A thrust fault propagates from calcareous light gray mudstone throughout the coaly black shale bedding, resulting in a fault propagation fold.

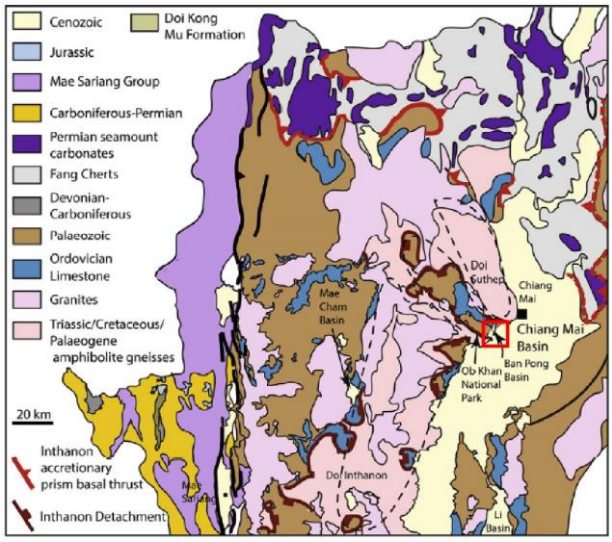

Figure 3 Geological map of NW Thailand presents Ban Pong Basin's location (a red rectangle) on the western side of the Chiang Mai Basin (modified from Gardiner et al. (2016); Morley and Racey (2011), and cited in Mankhemthong et al. (2019)).

The non-filtered samples were used to measure anions (e.g., Cl, SO_4,…) and some cations (e.g., Ca, Mg,…). Then, another non-filtered part was acidified with 35% HNO_3 to bring the pH close to 2 prior to measuring cations (e.g., Fe, Mn,…). Finally, the left sample was filtered using 45 µm syringe filter paper and then acidified with 35% HNO_3 to be preserved before measuring total arsenic (As).

3.2 Geochemical analyses

In the laboratory, the rock samples were dried in an oven at 40°C for 24 hours to remove moisture and then the samples were pulverized by a disc mill prior to further analyses. The mineral assemblages were analyzed by a Bruker X-ray Diffractometer (XRD) at the Department of Geology, Chulalongkorn University, Bangkok, Thailand, to identify the mineral compositions. Furthermore, the samples were also tested for geochemical analyses. Major and minor oxides were decided by a standardless analysis of a Bruker S4 X-ray Fluorescence (XRF) spectrometer at the Department of Geology, Chulalongkorn University. The loss on ignition (LOI) was measured from the weight differences between dried powder and after ignition at 1000°C for three hours in an electric furnace. In addition, the samples were prepared using the four-acid digestion method prior to identifying the trace elements by using Inductively Coupled Plasma-Mass Spectrometer (ICP-MS) at ALS laboratory in Australia.

3.3 Acid forming potential analyses

AMD potential can be estimated from acid forming potential (AFP) of the rocks, which is measured by using acid-base accounting (ABA) and net acid generation (NAG) tests (Assawincharoenkij et al., 2017).

The ABA is a statistical procedure evaluating the balance between the acid generation from sulfide mineral oxidation and acid-neutralizing from the dissolution of alkaline carbonate. The result will be reported in terms of net acid-producing potential (NAPP) (Eq.4) derived from the subtraction of acid-neutralizing capacity (ANC) from maximum potential acidity (MPA) (Ian Wark Research Institute, 2002; Miller and Jeffery, 1995).

$$NAPP = MPA - ANC \quad \text{.....(4)}$$

The maximum potential acidity is derived from the total sulfur content of the samples. The total sulfur is usually determined by a high-temperature combustion method and is typically assumed that occur from pyrite (FeS_2) oxidation (Changul et al., 2010b; Ian Wark Research Institute, 2002; Stewart et al., 2006). The total sulfur 1% is equal to 30.6 kilograms of H_2SO_4 per ton of material (kg H_2SO_4/t) (Miller and Jeffery, 1995).

The ANC test is used for measuring acid-neutralizing capacity from neutralizing minerals. The methodology followed a modified method of Sobek (1987), proposed by Ian Wark Research Institute (2002). The acid-neutralizing capacity is derived from back-titrating the mixture between the sample and the standardized hydrochloric acid (HCl) with sodium hydroxide (NaOH). The result will be reported in kg H_2SO_4/t.

The NAG test allows acid generation and acid neutralization to occur simultaneously (Ian Wark Research Institute, 2002). In addition, the test measures the final pH of the samples after the oxidation process of hydrogen peroxide (H_2O_2) and iron sulfide minerals (Assawincharoenkij et

al., 2017; Changul et al., 2010b; Miller, 1997). Stewart et al. (2006) proposed that the NAG test might help resolve uncertainties in ABA predictions.

The criteria to determine acid forming potential was suggested by Stewart et al. (2006) (Table 1). Samples are classified as potentially acid forming (PAF) if they have a positive NAPP and $NAG_{pH} < 4.4$, non-acid forming (NAF) if they have a negative NAPP and $NAG_{pH} \geq 4.4$, and uncertain (UC) when they reveal an obvious conflict between the NAPP and NAG_{pH} results.

Table 1 Criteria of acid forming potential classification suggested by Stewart et al. (2006).

Classification	Criteria
PAF	NAPP > 0 and $NAG_{pH} < 4.4$
NAF	NAPP ≤ 0 and $NAG_{pH} \geq 4.4$
UC	(NAPP ≤ 0 and $NAG_{pH} < 4.5$) or (NAPP > 0 and $NAG_{pH} \geq 4.5$)

3.4 Hydrochemical analyses

Water chemistry parameters of water samples were analyzed at the hydrochemical laboratory, the Department of Groundwater Resources, Bangkok, Thailand. Cu, Fe, Mn, and Zn concentrations were determined using an Atomic Absorption Spectrophotometer (AAS). The concentration of Ca, Mg, CO_3, and HCO_3 were defined using titration. A flame photometer identified Na and K concentrations. The concentration of Cl was measured by the argentometry titration method. The automated cadmium reducing method determined NO_2 and NO_3 concentration, while the automated methylthymol blue method characterized the concentration of SO_4. Finally, an ion-selective method and ICP-MS analysis resolved the F and As concentrations.

4. Results

4.1 Lithology

The lithostratigraphic log in Figure 4 was produced from the section of interest. An overall section thickness is approximately 8 meters. This section contains thick calcareous light gray mudstone and coaly black shale or black shale with fossil fragments interbedded with pale brown marlstone. The bedding thickness ranges between 0.6-2.5 m, 0.1-0.2 m, and 0.2-0.5 m for calcareous light gray mudstone, pale brown marlstone, and coaly black shale and black shale with fossil fragments, respectively. Moreover, some coaly black shale successions contain carbon film, plant fossils, fossil fragments, and mud clasts. Elemental sulfur is also observed on the weathering surface of coaly black shale. Regarding the acid effervescence, the pale brown marlstone and black shale with fossil fragments react vigorously with hydrochloric acid (HCl). On the other hand, calcareous light gray mudstone also slightly to moderately reacts with HCl, but no reaction is observed between coaly black shale and HCl.

4.2 Mineral assemblage

Based on the mineral assemblages analyzed by XRD analysis in Table 3, the calcareous light gray mudstone is abundant with quartz, muscovite, and calcite. Moreover, the pale brown marlstone predominantly comprises major calcite and minor pyrite. The coaly black shale mainly contains quartz and pyrite, but the black shale with fossil fragments primarily consists of quartz, calcite, and pyrite. Moreover, a small amount of siderite is contained in all rock types. Besides, gypsum is also noticed in coaly black shale and black shale with fossil fragments.

4.3 Bulk geochemistry

Regarding the major oxide result in Table 2, the rocks in the interval of interest mostly contain SiO_2, Al_2O_3, Fe_2O_3, and K_2O, in the range of 2.64-53.95, 1.31-17.43, 1.64-9.60, and 0.17-3.90 wt.%, respectively. Most rocks are dominated by SiO_2, except the pale brown marlstone and black shale with fossil fragments which are predominant with CaO (56.94 - 65.89 and 28.24 wt.%, respectively). On the other hand, the SO_3 tends to be abundant in the coaly black shale, black shale with fossil fragments, and pale brown marlstone (4.98-11.80, 6.21, 1.02-2.63 wt.%, respectively). Furthermore, more than 1.00 wt.% of MgO is reported in calcareous light gray mudstone.

In addition, trace element results in Table 2 are in the range of 2.84-229, 2.07- 31.10, 10.0-94.2, 0.102-3.490, 11.65-82.40, 2.37-53.40, 12.3-

186.5 ppm for As, Co, Cr, Cd, Ni, Pb, and Zn, respectively. The contents of As, Cr, and Pb are the most abundant in coaly black shale. Even though calcareous light gray mudstone is the most enriched with Ni and Zn concentration, it seems to contain less trace elements than other rocks.

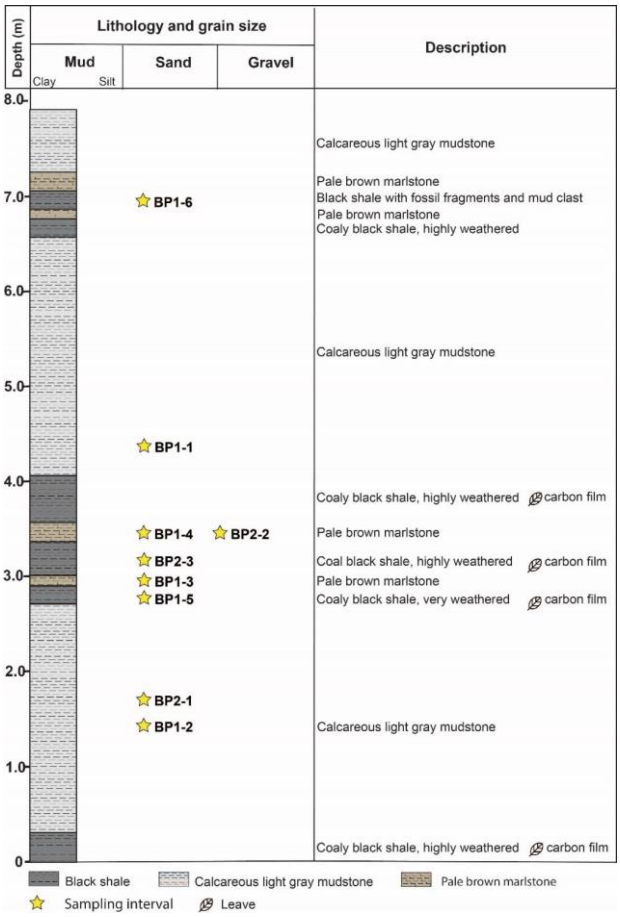

Figure 4 The lithostratigraphic log performed at the section of interest in Figure 2 shows that this section contains calcareous light gray mudstone, pale brown marlstone, coaly black shale, and black shale with fossil fragments. The interval of rock samples is also shown in this stratigraphic log.

4.4 Acid forming potential

The acid forming potential of the rock samples was classified based on ABA and NAG tests. The result of both tests is expressed in Table 4. Regarding the ABA test, total sulfur can be detected in samples BP1-4 of pale brown marlstone (0.05%), BP1-5 and BP2-3 of coaly black shale (2.04% and 0.34%, respectively), and BP1-6 of black shale with fossil fragments (1.05%). Consequently, these total sulfur proportions cause MPA values of 0.34, 2.04, 1.05, and 15.30 H_2SO_4/t for samples BP1-4, BP1-5, BP2-3, and BP1-6, respectively. On the other hand, the ANC results of all samples are displayed in the range of 3.55 – 1159.10 H_2SO_4/t. After subtracting MPA by ANC, the result shows positive NAPP for coaly black shale, indicating potentially acid forming (PAF). In contrast, other rocks demonstrate negative NAPP, leading to being characterized as non-acid forming (NAF).

Likewise, the NAG result shows that two samples of coaly black shale (BP1-5 and BP2-3) have NAG_{pH} of 1.54 and 2.54, respectively. Since these NAG_{pH} values are less than 4.4, the samples are classified as PAF. In contrast, the other rocks display NAG_{pH} higher than 4.4; consequently, they are characterized as NAF. In conclusion, based on a combination of these two tests, only the rock samples of coaly black shale (BP1-5 and BP2-3) are identified as PAF, whereas others are classified as NAF. The illustration of acid forming potential results is presented in Figure 5.

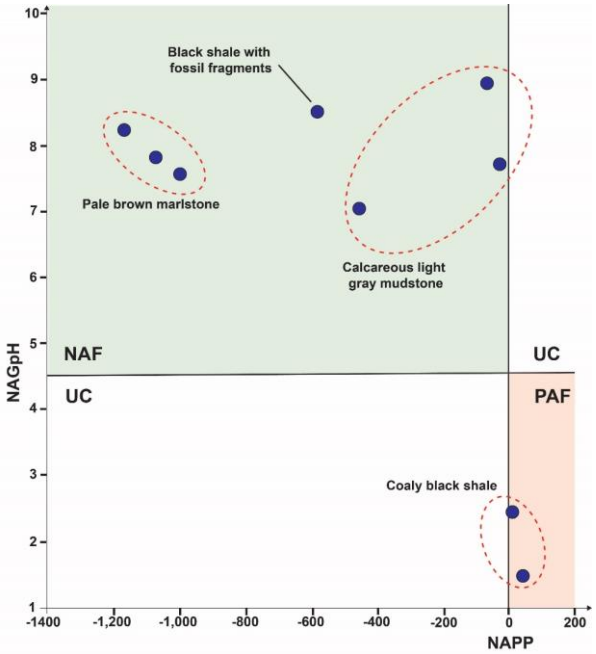

Figure 5 Acid forming potential of rock is presented in the graph plotted between NAPP and NAG_{pH}. Coaly black shale is classified as PAF, whereas other rocks are categorized as NAF.

Table 2 Major oxides (%) and trace elements (ppm) of rock samples from XRF and ICP-MS analyses.

Lithology	Calcareous light gray mudstone			Pale brown marlstone			Coaly black shale		Black shale with fossil fragments	Average shale*
Sample name	BP1-1	BP1-2	BP2-1	BP1-3	BP1-4	BP2-2	BP1-5	BP2-3	BP1-6	
SiO	50.26	30.04	53.95	3.21	2.64	6.39	25.93	41.54	18.98	
Al_2O	16.64	11.46	15.08	2.42	1.31	3.19	13.03	17.43	9.42	
FeO_3	5.55	6.36	8.23	1.64	3.03	4.48	9.60	5.27	7.29	
K_2O	3.90	2.70	3.05	0.27	0.17	0.48	2.45	3.31	1.88	
MgO	1.53	1.44	0.79	0.58	0.63	0.60	0.79	0.91	0.74	
CaO	0.90	25.04	1.82	65.60	65.89	56.94	1.57	0.41	28.24	
TiO_2	0.78	0.42	0.60	0.05	0.03	0.10	0.55	0.75	0.39	
P_2O_5	0.29	0.26	0.38	0.12	0.07	0.10	0.07	0.07	0.39	
MnO	0.28	3.26	1.02	0.36	0.69	0.23	0.02	0.11	0.31	
Na_2O	0.13	0.25	0.05	0.00	0.09	0.05	0.09	0.03	0.08	
SO_3	0.11	0.25	0.21	1.02	1.82	2.63	11.80	4.98	6.21	
LOI	0.07	0.24	0.08	0.41	0.39	1.08	0.58	0.21	0.39	
Total	80.44	81.71	85.26	75.68	76.75	76.26	66.48	75.00	74.30	
As	2.84	51.60	31.30	14.25	57.20	74.50	229.00	102.50	27.00	10
Co	29.70	31.10	14.20	2.27	2.07	3.93	6.94	13.45	10.30	19
Cr	67.4	43.1	60.8	14.2	10.0	22.7	71.4	94.2	55.6	90
Cd	0.378	3.490	0.226	0.226	0.102	0.505	0.343	0.709	0.175	0.8
Ni	78.20	82.40	32.90	11.65	12.20	20.70	39.40	63.00	41.20	68
Pb	51.50	48.10	38.20	6.48	2.37	16.95	20.00	53.40	18.65	20
Zn	186.5	102.5	76.1	20.8	12.3	32.4	59.8	132.5	57.2	160

Table 2 XRD analysis reveals mineral assemblages of each rock type.

Lithology	Calcareous light gray mudstone			Pale brown marlstone			Coaly black shale		Black shale with fossil fragments
Sample name	**BP1-1**	**BP1-2**	**BP2-1**	**BP1-3**	**BP1-4**	**BP2-2**	**BP1-5**	**BP2-3**	**BP1-6**
Quartz	***	**	***	*	*	*	***	***	***
Pyrite	-	-	-	*	*	*	***	**	***
Calcite	-	***	*	***	***	***	-	-	***
Gypsum	-	-	-	-	*	*	*	*	-
Chlorite	**	-	-	-	-	-	*	*	*
Siderite	-	*	-	-	*	-	*	-	*

The degree of mineral abundance is presented as ***** Minor, ****** Moderate, ******* Dominant

Table 3 Classification of the acid forming potential of rock exposure at the open-pit mine, Ban Pong Basin.

Sample name	**Lithology**	**ABA Test**					**NAG Test**		**Classification**
		Total Sulfur (%S)	**MPA** (kg H_2SO_4/t)	**ANC** (kg H_2SO_4/t)	**NAPP** (kg H_2SO_4/t)	**AFP**	**NAG pH**	**AFP**	
BP1-1	Calcareous light gray mudstone	LLD	0.00	29.68	-29.68	NAF	8.12	NAF	NAF
BP1-2		LLD	0.00	581.45	-581.45	NAF	8.93	NAF	NAF
BP2-1		LLD	0.00	70.19	-70.19	NAF	9.37	NAF	NAF
BP1-3	Pale brown marlstone	LLD	0.00	1159.10	-1159.10	NAF	8.65	NAF	NAF
BP1-4		0.50	15.30	1085.23	-1069.93	NAF	8.20	NAF	NAF
BP2-2		LLD	0.00	997.03	-997.03	NAF	7.93	NAF	NAF
BP1-5	Coaly black shale	2.04	62.42	16.78	45.64	PAF	1.54	PAF	PAF
BP2-3		0.34	10.40	3.55	6.85	PAF	2.54	PAF	PAF
BP1-6	Black shale with fossil fragments	1.05	32.13	483.88	-451.75	NAF	7.38	NAF	NAF

Classification of acid forming potential is based on criteria suggested by Stewart et al. (2006).

ABA test: acid-base accounting test, NAG test: net acid generation test

LLD: lower than the limit of detection, MPA: maximum producing acidity, ANC: acid neutralizing capacity, NAPP: net acid producing potential, AFP: acid forming potential

NAF: non-acid forming, PAF: potentially acid forming

Table 4 Physio-chemical parameters of surface water samples collected from upstream, mine water, and downstream.

Physio-chemical parameter (ppm)	BP-SW-01 Pond Upstream	BP-SW-02 Pond Mine water	BP-SW-03 River Downstream	TSWS*	TIES**
pH	8.52	6.98	7.65	5.0-9.0	5.5-9.0
TDS	180	543	208		<3,000
Ca	35	130	51		
Mg	14.0	36.0	6.5		
Na	2.4	2.0	9.6		
K	5.5	13.0	4.1		
Fe	0.1	0.1	0.5		
Mn	0.0	0.8	0.3	<1.0	< 5.0
Cu	0.0	0.0	0.1	<0.1	< 2.0
Zn	0.0	0.0	0.0	<1.0	< 5.0
SO_4	13	480	10		
Cl	2.0	1.6	5.2		
CO_3	0	0	0		
HCO_3	172	23	202		
F	1.1	0.5	0.4		
NO_2	0.00	0.03	0.00		
NO_3	1.2	0.1	1.1	<5.0	
As	<0.0028	<0.0028	<0.0028	<0.01	<0.25
Na/Na+Ca	0.18	0.10	0.21		
Cl/Cl+HCO_3	0.01	0.07	0.03		

*'Thailand's surface water standard is based on the Department of Pollution Control.
**'Thailand's industrial effluent standard is based on the Department of Pollution Control.

4.5 Water chemistry

Regarding the chemical parameters of water samples displayed in Table 5, water pH ranges from 6.98-8.52, while the TDS varies between 180-543 mgL^{-1}. The dominant cations from upstream are Ca and Mg (35 and 14.0 mgL^{-1}, respectively). Similarly, the essential cations in mine water are also Ca and Mg (130 and 36.0 mgL^{-1}, respectively). On the other side, the significant cations in a downstream water sample are Ca and Na (51 and 9.6 mgL^{-1}, respectively). However, for the anion, both the upstream and downstream water samples are predominant with HCO_3 (172 and 202 mgL^{-1}, respectively). In contrast, mine water is dominant with SO_4 (480 mgL^{-1}). Besides, no significant rise of any metal concentration is observed, except for increasing Mn concentration within the mine water and downstream samples. All water samples contain less than 0.0028 mgL^{-1} of As.

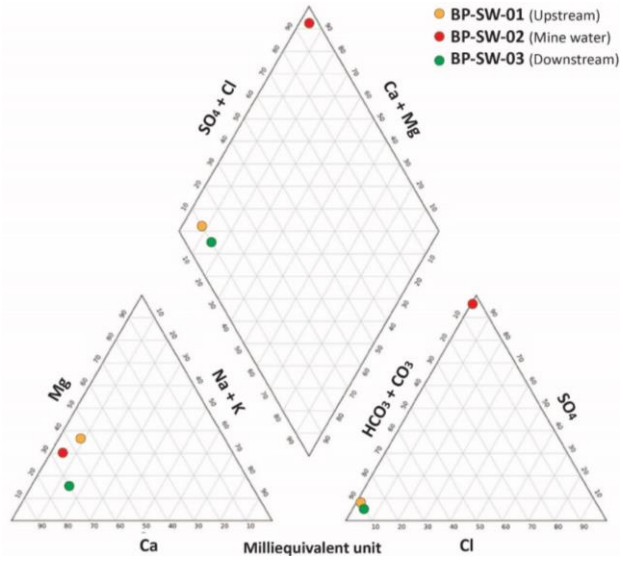

Figure 6 Hydrochemical facies of surface water collected in the BPB. The upstream and downstream are classified as Ca-Mg-HCO_3 type, whereas mine water is categorized as Ca-Mg-SO_4 type.

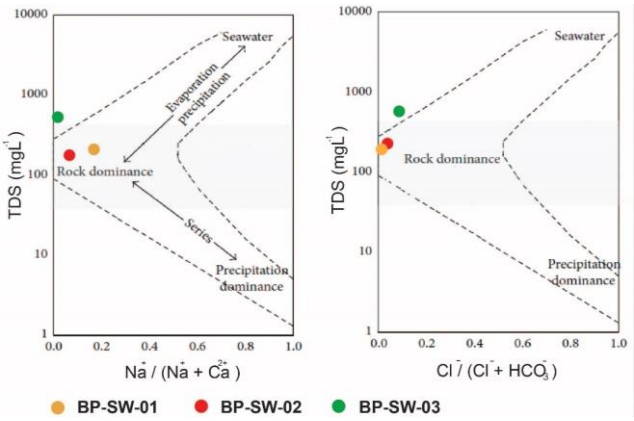

Figure 7 Gibb's diagram presents that the weathering of surrounding rocks controls water chemistry in the BPB.

In addition, Piper's diagram results (Fig. 6) reveal two hydrochemical facies of water: (1) Ca-Mg-HCO_3 type for upstream and downstream and (2) Ca-Mg-SO_4 type for mine water. Moreover, Gibb's diagram outcomes (Fig. 7) present that the weathering of rocks in the study area plays a significant role in the water chemistry in the study area.

5. Discussions

5.1 Acid forming potential

Regarding acid forming potential classification, only coaly black shale is classified as acid forming rock because its acid generation capability is higher than its acid neutralization capacity (see Table 4). The main acid generator for coaly black shale is pyrite in its composition. Sulfide minerals, including pyrite, in sedimentary rock typically form in highly-reducing sedimentary and diagenetic environments (Berner, 1984; Schoonen, 2004) as a result of sulfate-reducing bacteria's activities (Greenwood et al., 2013). Moreover, based on the XRD result, pyrite is also essentially noticed in black shale with fossil fragments and slightly detected in pale brown marlstone. However, pale brown marlstone primarily contains calcite as the main composition, and black shale is enriched with fossil fragments, acting as a source of carbonate mineral; these lead to acid neutralization capacity exceeding acid generation ability. As a result, the black shale with fossil fragments and pale brown marlstone are characterized as non-acid forming rocks. Similarly, other rocks are also considered non-acid forming rocks due to no pyrite and/or a large proportion of calcite minerals in their composition.

Moreover, to estimate AMD potential, Parviainen and Loukola-Ruskeeniemi (2019) suggested that, in addition to black shale's chemical composition and mineralogy, the volume of the black shale succession and the chemical composition of the surrounding rocks also need to be considered. Although the coaly black shale can produce the acid, its thickness is less than 1 meter and it is surrounded by calcite-rich rocks, including calcareous light gray mudstone and pale brown marlstone, which considerably provide acid neutralization capacity. Therefore, it can be assumed that the coaly black shale succession in the Ban Pong Basin has a low potential for acid mine drainage generation.

Additionally, compared to the average trace element in shale (see Table 2) suggested by Wedepohl (1971), the concentration of As in the coaly black shale (102.50-229.00 ppm) are ten to twenty times higher than that of the average shale (10 ppm). In addition to this, the concentration of Cr (94.2 ppm) and Pb (53.4 ppm) in the coaly black shale are also higher than the average value in the average shale (90.0 and 20.0 ppm for Cr and Pb in an average shale, respectively). Since coaly black shale is an acid forming rock, these trace elements might be released into the environment, leading to environmental impacts in the future. Likewise, the soil should not be produced from the succession of coaly black shale, as it might contain a significant level of hazardous trace elements, possibly harming natural creatures and humans.

According to the XRD result, some rock samples contain a small quantity of gypsum and siderite, which can cause uncertainty in the ABA test (Parbhakar-Fox and Lottermoser, 2015; Stewart et al., 2006). Gypsum is a calcium sulfate mineral ($CaSO_4.2H_2O$) that can increase the total sulfur, leading to the MPA overestimation. On the other hand, siderite is an iron carbonate mineral ($FeCO_3$) that can act as an acid neutralizer, causing an overrated ANC result (Blowes et al., 2014; Stewart et al., 2006).

5.2 AMD potential and hydrochemical characteristics of mine water

Regarding the result of physio-chemical parameters of mine water (a sample BP-SW-02) in the BPB, the pH of water is slightly neutral (pH 6.98). The water has low metal anions (Fe, Mn, Cu, Zn) and As but slightly high sulfate (SO_4) concentration. The characteristics of the mine water are clearly conflicted with the common characteristics of AMD, which typically have acidic pH and high concentrations of sulfate (SO_4), iron (Fe), aluminum (Al), and trace elements (Blowes et al., 2014). According to this, therefore, the mine water at the open-pit mine in the Ban Pong Basin does not have the potential to become AMD. Moreover, a small amount of As in the water is not harmful to aqueous biota and humans because it is lower than the standard of surface water and industrial effluent (see Table 5).

The hydrochemical facies results of surface water indicate that the Ca, Mg, and HCO_3 are enriched in the surface water around the study area, while SO_4 is abundant in mine water. The dominance of Mg, Ca, and HCO_3 concentration in the surface water might be caused by weathering of carbonate material from the surrounding rocks, which mainly contain a high amount of carbonate mineral in their composition. This is supported by Gibb's diagram result that the weathering of surrounding rocks mainly controls water chemistry in the Ban Pong Basin. Besides, the elevated SO_4 in the mine water is possibly caused by pyrite oxidation (Lottermoser, 2010) within coaly black shale, black shale with fossil fragments, and pale brown marlstone, and gypsum dissolution.

6. Conclusion

The rock and water samples collected from the open-pit mine in the Ban Pong Basin, Chiang Mai province, are examined with geochemical and hydrochemical analyses to evaluate acid forming potential and acid mine drainage potential, respectively. Consequently, the following summarizations can be made:

1. Coaly black shale is the only acid forming rock in the study area. However, it has a low potential for generating acid mine drainage as it has a thin succession and is surrounded by calcite-rich rocks, which act as the acid neutralizer. However, since coaly black shale contains high concentrations of As, Cr, and Pb, these trace elements might be released into the environment or they might contaminate the soil produced from this mine.

2. The mine water does not have the potential to become AMD. The mine water, however, presents a high SO_4 concentration, which might be attributed to sulfide oxidation and gypsum dissolution. Additionally, the water bodies in the Ban Pong Basin tend to be plentiful with Ca, Mg, and HCO_3 derived from surrounding rock weathering.

7. Acknowledgment

The authors are very grateful to Assistant Professor Dr. Piyaphong Chenrai at the Department of Geology, Faculty of Science, Chulalongkorn University, for his assistance and suggestion during field data collection. Moreover, we would like to thank the Petroleum Geoscience Program, Department of Geology, Faculty of Science, Chulalongkorn University for financial support of this research project. Finally, thanks are extended to the editors and anonymous reviewers for improving the manuscript.

8. Reference

Adisaipattanakul, N., 2014. Orientation and depositional environment in Cenozoic basin in Tambon Ban Pong and Tambon Nam Phrae, Hang Dong District, Chiang Mai Province. Independent study Thesis, Department of Geological Sciences, Faculty of Science, Chiang Mai University, 48 pp.

Assawincharoenkij, T., Hauzenberger, C. and Sutthirat, C., 2017. Mineralogy and geochemistry of tailings from a gold mine in northeastern Thailand. Human and Ecological Risk Assessment: An International Journal, 23(2): 364-387.

Berner, R.A., 1984. Sedimentary pyrite formation. Geochimica et Cosmochimica Acta, 48: 605–615.

Blowes, D.W., Ptacek, C.J., Jambor, J.L., Weisener, C.G., Paktunc, D., Gould, W.D. and Johnson, D.B., 2014. The Geochemistry of Acid Mine Drainage. Elsevier, pp. 131-190.

Changul, C., Sutthirat, C., Padmanahban, G. and Tongcumpou, C., 2010a. Assessing the acidic potential of waste rock in the Akara gold mine, Thailand. Environmental Earth Sciences, 60(5): 1065-1071.

Changul, C., Sutthirat, C., Padmanahban, G. and Tongcumpou, C., 2010b. Chemical characteristics and acid drainage assessment of mine tailings from Akara Gold mine in Thailand. Environmental Earth Sciences, 60: 1583–1595.

Equeenuddin, S.M., Tripathy, S., Sahoo, P.K. and Panigrahi, M.K., 2010. Hydrogeochemical characteristics of acid mine drainage and water pollution at Makum Coalfield, India. Geochemical Exploration, 105(3): 75-82.

Gardiner, N.J., Roberts, N.M.W., Morley, C.K., Searle, M.P. and Whitehouse, M.J., 2016. Did Oligocene crustal thickening precede basin development in northern Thailand? A geochronological reassessment of Doi Inthanon and Doi Suthep. Lithos 240–243: 69–83.

Greenwood, P.F., Brocks, J.J., Grice, K., Schwark, L., Jaraula, C.M.B., Dick, J.M. and Evans, K.A., 2013. Organic geochemistry and mineralogy I. Characterisation of organic matter associated with metal deposits. Ore Geology Reviews, 50: 1-27.

Huyck, H.L.O., 1990. When is a metalliferous black shale not a black shale? In: R.I. Grauch, Huyck, H.L.O. (Editor), Metalliferous Black Shales and Related Ore Deposits. U.S. Geological Survey, United States Working Group Meeting, Denver, International Geological Correlation Program Project 254, pp. 42–56.

Ian Wark Research Institute, E.G.I., 2002. ARD Test Handbook. Prediction and Kinetic Control of Acid Mine Drainage. AMIRA International, Melbourne.

Jambor, J.L., Dutrizac, J.E. and Chen, T.T., 2000. Contribution of Specific Minerals to the Neutralisation Potential in Static Tests, The Fifth International Conference on Acid Rock Drainage. Society for Mining, Metallurgy and Exploration Inc., Littleton., Denver Colorado, pp. 551-565.

Kontinen, A., Hanski, E., 2015. Other types of mineral deposits, Mineral Deposits of Finland, pp. 557-611.

Kwong, Y.T.J., Whitley, G. and Roach, P., 2009. Natural acid rock drainage associated with black shale in the Yukon Territory, Canada. Applied Geochemistry, 24(2): 221-231.

Lottermoser, G.B., 2010. Mine Wastes Characterization, Treatment and Environmental Impacts. Springer, 410 pp.

Mankhemthong, K., Morley, C.K., Takaew, P. and Rhodes, B.P., 2019. Structure and evolution of the Ban Pong Basin, Chiang Mai Province, Thailand. Journal of Asian Earth Sciences, 172: 208-220.

Miller, S. and Jeffery, J., 1995. Advances in the Prediction of Acid Generating Mine Waste Materials. In: N.J. Grundon and L.C. Bell (Editors), The Second Australian Acid Mine Drainage Workshop Australian Centre for Minesite Rehabilitation Research, Brisbane, pp. 33-43.

Miller, S., Robertson, A., and Donohue, T. , 1997. Advances in Acid Drainage Prediction Using the Net Acid Generation (NAG) Test, The 4th International Conference on Acid Rock Drainage Vancouver, pp. 535-549.

Morley, C.K. and Racey, A., 2011. Tertiary stratigraphy. In: M.F. Ridd, A.J. Barber and M.J. Crow (Editors), Geology of Thailand,. Geological Society London, pp. 223–271.

Nordstrom, D., Southam, G., 1997. Geomicrobiology of sulfide mineral

oxidation. Mineral. Geochem., 35: 61–390.

Parbhakar-Fox, A. and Lottermoser, B., G. , 2015. A critical review of acid rock drainage prediction methods and practices. Minerals Engineering, 82: 107-124.

Parviainen, A. and Loukola-Ruskeeniemi, K., 2019. Environmental impact of mineralised black shales. Earth-Science Reviews, 192: 65-90.

Schoonen, M.A.A., 2004. Mechanisms of sedimentary pyrite formation. Geological Society of America Special Papers, 379: 117-134.

Sobek, A.A., Schuller, A. W., Freeman, R. J., Smith, M. R., 1987. Field and Laboratory Methods Applicable to Overburdens and Minesoils, U.S. Environmental Protection Agency, Cincinnati, Ohio.

Stewart, W.A., Miller, S.D. and Smart, R., 2006. Advance in Acid Rock Drainage (ARD) characterisation of mine waste. In: M.O. St. Louis and R.I. Barnhisel (Editors), the 7th International Conference on Acid Rock Drainage (ICARD). the American Society of Mining and Reclamation (ASMR), 3134 Montavesta Road, Lexington, KY 40502, pp. 2098-2119.

Strosnider, W.H.J., Llanos López, F., Nairn, R., 2011a. Acid mine drainage at Cerro Rico de Potosí I: unabated high-strength discharges reflect a five century legacy of mining. Environmental Earth Sciences, 64: 899–910.

Strosnider, W.H.J., Llanos López, F., Nairn, R., 2011b. Acid mine drainage at Cerro Rico de Potosí II: severe degradation of the Upper Rio Pilcomayo watershed. Environmental Earth Sciences, 64: 911–923.

Sun, J., Tang, C., Wu, P., Strosnider, W.H.J. and Han, Z., 2013. Hydrogeochemical characteristics of streams with and without acid mine drainage impacts: A paired catchment study in karst geology, SW China. Journal of Hydrology, 504: 115-124.

Wedepohl, K.H., 1971. Environmental influences on the chemical composition of shales and clays. Physics and Chemistry of the Earth, 8: 307-333.

Wignall, P.B., 1994. Black Shales, Clarendon Press, Oxford., 127 pp.